



Coherent backscattering of light by an anisotropic biological network

Gianni Jacucci¹, Olimpia D. Onelli¹,
Antonio De Luca^{2,3}, Jacopo Bertolotti⁴,
Riccardo Sapienza^{5,*}, and Silvia Vignolini

1

¹ Department of Chemistry, University of Cambridge, Lensfield Road, Cambridge, CB2 1EW, United Kingdom ² Department of Physics, University of Calabria, Rende (CS), via Pietro Bucci, 87036, Italy ³ National Research Council, Institute of Nanotechnology, SS Cosenza, via Pietro Bucci, 87036, Italy ⁴ Department of Physics and Astronomy, University of Exeter, Stocker Road, Exeter, EX4 4QL, United Kingdom ⁵ The Blackett Laboratory, Department of Physics, Imperial College London, London SW7 2BW, United Kingdom * Corresponding Author: r.sapienza@imperial.ac.uk

The scattering strength of a random medium relies on the geometry and spatial distribution of its components as well as on their refractive index. Anisotropy can therefore play a major role in the optimisation of the scattering efficiency both in biological and synthetic materials. In this work, we show that by exploiting the coherent backscattering phenomenon it is possible to characterise the optical anisotropy in the *Cyphochilus* beetle scales without the need of changing their orientation or their thickness. For this reason, such a static and easily accessible experimental approach is particularly suitable for the study of biological specimens. Moreover, the estimation of the anisotropy in the *Cyphochilus* beetle scales might provide inspiration for improving the scattering strength of artificial white materials.

1. Introduction

An object is opaque white when the light incident on it undergoes multiple scattering events before exiting the medium, *i.e.* when the object is optically thick. [1] The optical thickness is defined as the ratio between the physical thickness of an object and the transport mean free path (ℓ_t), namely the distance that light travels before losing information about its starting propagation direction [2, 3]. Commonly, ℓ_t is of the order of tens of microns in low-refractive index white materials. [4, 5] Therefore, opacity is only achieved for relatively large thicknesses (of the order of hundreds of microns) to allow a sufficient number of scattering events.

Nature, however, provides a different approach that can serve as an inspiration for the manufacturing of polymeric, thin but still opaque white materials. [6, 7, 8] In particular, the brilliant whiteness shown by the *Cyphochilus* beetle is known to be generated by multiple scattering of light inside the extremely thin scales ($\simeq 7\ \mu\text{m}$ thick) that cover its exoskeleton (Figure 1a-b). [4, 9, 10, 11, 12] The beetle intra-scale structure is composed of a nanostructured network of chitin filaments with a filling fraction of around 45%. [13] The chitin fibers inside the beetle scales are organised anisotropically, *i.e.* mainly oriented parallel to the surface of the scales (Figure 1c). This structural anisotropy increases the scattering strength in the orthogonal direction to the scale surface, at expense of the in-plane scattering, which is not as relevant for the total reflectance of the insect. [12] With such morphology and geometry, the beetle achieves a high total reflectance (about 70% over the whole visible range) with a thin, lightweight, and anisotropic network made of low refractive index material. [4, 12, 13]

In the recent years a number of different techniques have been used to characterise anisotropic media, for example, spatially resolved reflectance, [14, 15] imaging diffuse transmission, [12, 16, 17] spatio-temporal visualisation of transmitted light, [18] and coherent backscattering. [19, 20, 21, 22] As of yet, the accuracy in the determination of the in-plane and out-of-plane components of the light transport mean free path in the *Cyphochilus* beetle scales has been limited by the strong thickness dependency of the experimental techniques used. [4, 12]

In this work, we show that the coherent backscattering technique is well suited for studying the scattering properties of biological samples, allowing to estimate the anisotropy of a system without the need of changing its orientation and its thickness. Moreover, the CBS provides a precise evaluation of the in-plane transport mean free path without requiring samples with different thicknesses, in contrast with other static and easily accessible techniques. Our experimental results contribute to the understanding of scattering optimisation in the *Cyphochilus* beetle scales, providing a valuable guide for the development of novel sustainable materials by

35 showing how to obtain a strong optical response whilst using a low-refractive index biopolymer
36 as building block.

37 2. Results and Discussion

38 To characterise light propagation in the *Cyphochilus* scales, we performed a coherent
39 backscattering (CBS) experiment. We measured the angular resolved light scattered by the sample
40 around the backscattering direction, which shows a characteristic peak profile. [23] The CBS is
41 the Fourier transform of the spatial distribution of light exiting the sample in the backscattering
42 direction. [3] This phenomenon is often understood as an interference effect that originates from
43 the superposition of a large number of two-wave interference patterns from reciprocal waves.
44 [23, 24, 25, 26, 27] These waves have traveled the same optical path inside the medium but
45 in opposite directions (Figure 2a) and are therefore phase-related. The resulting CBS intensity
46 distribution has a conical shape whose width provides a direct measurement of the light transport
47 mean free path of a material. [3]

48 The experimental setup is shown in Figure 2b. A collimated laser diode (peak wavelength
49 at 635 nm, spot-size of 2.5 mm, and output power of 1.2 mW) was used as light source. The
50 scattered signal was focused, using a parabolic mirror, on a 100 μm core fiber connected to a
51 spectrometer. The angular resolution of our setup was $\simeq 0.25$ mrad. To acquire the CBS line shape,
52 the speckle pattern, which occurs due to the high spatial coherence of the light source, needs to be
53 averaged out. [26] This was done by placing the sample on a motorised rotation mount whose axis
54 was the same of the propagation direction of the incoming laser beam. This averaging procedure
55 precludes the possibility to investigate a potential in-plane, xy , anisotropy. However, it has been
56 recently shown that the *Cyphochilus* scales are characterised by an isotropic spectral density in the
57 xy plane. [13] For this reason, our work focused only on the study of an out-plane anisotropy.

58 The enhancement factor of the coherent signal, *i.e.* the ratio between the intensity at exact
59 backscattering angle and the incoherent background, strongly depends on the polarisation. This
60 is maximised when the single-scattered photons, which do not have a reciprocal counterpart
61 and therefore contribute only to the incoherent background, are filtered out. This can be done
62 by acquiring the CBS in the *helicity conserving channel* (HC) (Figure 2). The HC signal was then
63 normalised to the one acquired in a *linear non conserving* (LNC) configuration, as discussed in Ref.
64 [28].

65 The measured CBS signal is reported in Figure 3. The experimental data show a maximum
66 lower than the theoretical value for semi-infinite media of 1 and a rounded top. This deviation
67 is a consequence of the small thickness of the *Cyphochilus* scales and can be described by the
68 isotropic theory for finite media: [29]

$$\begin{aligned}
\gamma_c = & 3e^{-b\nu} \left[\cos(bu) \left[\left(\frac{(\nu - (\nu - \alpha) \cosh(2z_e \alpha))}{(\nu - \alpha)^2 + u^2} \right) + \left(\frac{(\nu - (\nu + \alpha) \cosh(2z_e \alpha))}{(\alpha + \nu)^2 + u^2} \right) \right] \right. \\
& + \sin(bu) \left(\frac{u}{(\alpha + \nu)^2 + u^2} - \frac{u}{(\nu - \alpha)^2 + u^2} \right) \sinh(2z_e \alpha) \\
& + \frac{(\nu - \alpha) \cosh((\nu - \alpha)b - 2z_e \alpha) - \nu \cosh((\nu - \alpha)b)}{(\nu - \alpha)^2 + u^2} \\
& \left. + \frac{(\nu + \alpha) \cosh((\nu + \alpha)b - 2z_e \alpha) - \nu \cosh((\nu + \alpha)b)}{(\alpha + \nu)^2 + u^2} \right] \quad (2.1)
\end{aligned}$$

69 where $\mu = \cos(\theta)$, $\nu = \frac{1}{2}(1 + \frac{1}{\mu})$, $u = k\ell_t(1 - \mu)$, $\alpha = k\ell_t \sin(\theta)$, $B = b + 2z_e$. The parameters k ,
70 ℓ_t , and b are the wave vector, the isotropic transport mean free path, and the optical thickness,
71 respectively. For semi-infinite media, *i.e.* $b \rightarrow \infty$, Equation 2.1 reduces to: [29]

$$\gamma_{c,semi} = \frac{3 \left[\alpha + \nu \left(1 - e^{-2z_e \alpha} \right) \right]}{2\alpha\mu\nu \left[(\alpha + \nu)^2 + u^2 \right]} \quad (2.2)$$

72 The reduction of the theoretical maximum in finite media is caused by the suppression of long
73 light paths, which are responsible for the formation of the cusp of the CBS profile for semi-
74 infinite media. [2] To accurately determine the transport mean free path, the effect of the internal
75 reflections at the scale interface on the light path distribution inside the chitin network was
76 accounted in the extrapolation length $z_e = (2/3)(1 + R)/(1 - R)$. [30, 31, 32] R is the angle-
77 and polarisation-averaged reflection coefficient at the slab interface and can be obtained by an
78 angular integration of the Fresnel's coefficients. [31, 33] These coefficients depend on the effective
79 refractive index (n_e) of the chitin network, which was estimated by the Maxwell-Garnett's theory.
80 [34] The expression of z_e used in this work, and in the related literature regarding the study of the
81 *Cyphochilus* beetle, is the one derived for isotropic systems. This approximation is justified by the
82 absence of an analytical formula of the extrapolation length in anisotropic media. [35]

83 Using a filling fraction of $(45 \pm 6)\%$, [13] we calculated that $n_e = (1.22 \pm 0.03)$, $R = (0.32 \pm$
84 $0.04)$, and $z_e = (1.29 \pm 0.11)$. Finally, using the extrapolation length found from the expression
85 above, we obtained $\ell_t = (1.40 \pm 0.09) \mu\text{m}$ from the fit shown in Figure 3.

86 In the literature, the isotropic theory has been used to obtain information about media where
87 the anisotropy is in the plane perpendicular (xy) to the incoming beam (z direction). [19, 36] This
88 type of anisotropy gives rise to a CBS cone whose line shape differs when acquired along the
89 x and y directions. [36] It has been recently shown that the isotropic theory cannot be used to
90 obtain quantitatively reliable information about the anisotropic light transport along perpendicular
91 directions. [35] However, the anisotropy can be qualitatively estimated as the ratio between the
92 widths of the CBS line shapes acquired along the x and y directions, which can be individually
93 described by the isotropic theory. [36] Similarly, in the case of birefringent media as nematic liquid

94 crystals, the isotropic theory can be used to describe the CBS line shapes originating from different
95 polarisation configurations. [19]

96 In the case of the *Cyphochilus* beetle, the anisotropy is in the xz - and yz -plane (defining z
97 as perpendicular to the surface of the scales) [12, 13] and therefore the resulting CBS profile is
98 isotropic (for light incoming along the z direction). Due to the particularly small thickness of the
99 scales ($\simeq 7 \mu\text{m}$), the probing direction of the incoming beam cannot be changed.

100 As the anisotropy cannot be investigated directly, to gain insight on the light transport inside
101 the scales we performed anisotropic Monte Carlo simulations for scalar waves. A Monte Carlo
102 technique is well suited for describing light propagation in disordered media, where the photons
103 paths can be mathematically mapped into random walks. [2, 3, 37] Monte Carlo simulations
104 have been extensively used both to investigate theoretical aspects of anisotropic diffusion,
105 [14, 35, 38, 39, 40, 41] and to accurately describe experimental results regarding light propagation
106 in anisotropic media. [15, 19, 22]

107 Here, the photons paths in the white beetle scales were modeled by a series of random
108 steps. [42] The anisotropy of the system was introduced *via* a direction-dependent step size,
109 *i.e.* the components of the step vector were sampled from two different negative exponential
110 distributions with mean ℓ_{xy} and ℓ_z for the in-plane and out-of-plane components, respectively.
111 The angular component of each of the random steps was sampled from a distribution of points
112 uniformly distributed on the surface of a unit sphere. [43, 44] The collection of the initial and
113 final positions of the walkers that escaped the material from the same face they entered it,
114 that corresponds to reflected photons, was then used to reconstruct the CBS line shape. [3, 29]
115 The effect of residual absorption on the CBS line shape is not considered, due to the negligible
116 absorption of chitin in the visible. [45] The only parameters required for our Monte Carlo
117 simulations are the random steps distribution, the scales thickness and the reflection coefficient
118 at the scale interface (R). A schematic of the simulations parameters is illustrated in Figure 4a.

119 Figure 4b-c show how the CBS line shape is affected both by changing the in-plane (ℓ_{xy})
120 and out-of-plane (ℓ_z) components of the transport mean free path. In particular, ℓ_{xy} determines
121 the width of the CBS profile, while the optical thickness, defined as $OT = L/\ell_z$ (where L is the
122 thickness of the medium), specifies the enhancement of the coherent signal. These results can
123 be qualitatively explained by the fact that the CBS depends only on the distance between the
124 positions of the first scattering event (when the photon enters the medium) and the last (when the
125 photon exits the medium). When a large number of photons is considered, these two positions
126 have on average the same z coordinate (which is of the order of ℓ_z) and therefore their distance
127 can be considered to be z -independent. However, as discussed previously for the isotropic theory,
128 when the optical thickness of the medium is small (*i.e.* when long light paths are not allowed

129 by the finite thickness of the medium) the top of the CBS is rounded. The limited influence of
 130 the optical thickness on the width of the CBS line shape allows to obtain a precise value of ℓ_{xy}
 131 without requiring samples with different thicknesses. By fitting the experimental data with the
 132 Monte Carlo simulations, it is possible to disentangle the contribution of ℓ_{xy} and ℓ_z to the CBS
 133 line shape. In particular, we obtained a value of $\ell_{xy} = (1.40 \pm 0.09) \mu\text{m}$ and an optical thickness
 134 $OT = (6.89 \pm 0.13)$. The data were fitted by minimising the χ^2 . The errors in ℓ_{xy} and OT were
 135 estimated by performing simulations where the two parameters were gradually changed. This
 136 procedure was then repeated for taking into account the uncertainty in the determination of
 137 reflection coefficient (R).

138 The measured optical thickness is in good agreement with the total transmission data reported
 139 in the literature. [4, 12] The total transmission (T) for slab geometry media in the diffusion
 140 approximation is:

$$T = \frac{2z_e}{L + 2z_e}, \quad (2.3)$$

141 where L is the slab thickness. Equation 2.3 is the limit for negligible absorption of the expression
 142 derived in Ref. [46]. Using $T = (0.29 \pm 0.02)$, as reported in Ref. [4, 12], and the extrapolation
 143 length previously calculated we obtained $OT_{lit} = (6.3 \pm 1.2)$, consistent with what we measured.

144 From the measured OT and assuming $L = (7 \pm 1) \mu\text{m}$, where L and its error represent the
 145 mean and 1σ of the distribution reported in Ref. [12], we obtained $\ell_z = (1.02 \pm 0.15) \mu\text{m}$. The
 146 error in ℓ_z , which is mainly determined by the uncertainty in the thickness of the sample, can be
 147 affected by systematic errors given by surface roughness and curvature. [3, 47, 48]

148 Comparing ℓ_z with ℓ_{xy} , the measured optical anisotropy (OA) is:

$$OA = \frac{\ell_{xy} - \ell_z}{\ell_z} = (0.37 \pm 0.24). \quad (2.4)$$

149 Our experimental result is in agreement with the 3D reconstruction of the chitin network reported
 150 in Ref. [13], which predicts $OA \simeq 0.5$.

151 3. Conclusions

152 In conclusion, we demonstrated that the transport mean free path and optical anisotropy of
 153 light in the *Cyphochilus* beetle scales can be determined by measuring the CBS and that the
 154 results are in agreement with the one predicted in Ref. [13]. Exploiting the CBS effect provides a
 155 measurement of the optical anisotropy which describes more accurately the scattering properties
 156 of the *Cyphochilus* beetle compared to the results reported in the literature. In addition, the
 157 experimental technique reported here allows to estimate the anisotropy of a system without
 158 the need of changing its orientation and its thickness, making the CBS a technique particularly
 159 suitable for the study of biological specimens.

160 Authors Contribution.

161 G.J., O.D.O., A.D.L., R.S., and S.V. designed the experiments. G.J., J.B., R.S., and S.V. conceived
162 and planned the simulations. G.J. carried out the experiments and the simulations. All authors
163 provided critical feedback and helped shape the research, analysis and manuscript.

164 Acknowledgements.

165 G.J. thanks A. Lopresti, S.R. Hinestrosa, L. Barberi, and A. Caputo, and for the fruitful discussions
166 and advices on numerical methods. G.J. and O.D.O thank Dr. V.E. Johansen, R. Middleton, Dr. G.
167 Palermo and Dr. G. Kamita for their assistance on experimental techniques.

168 Data Accessibility.

169 The raw data and the Monte Carlo code regarding the publication can be found on the online
170 figshare repository.

171 Funding.

172 This work was supported by the European Research Council [ERC-2014-STG H2020 639088], the
173 BBSRC David Phillips Fellowship [BB/K014617/1], the EPSRC [EP/L016087/1, EP/L015978/1,
174 EP/N016920/1], the Leverhulme Trust's Philip Leverhulme Prize and the Leverhulme Trust (No.
175 RPG-2016-129), the EPSRC (grant nos. EPSRC EP/M027961), the Leverhulme Trust (No. RPG-
176 2014-238), the Royal Society (No. RG140457), and the Nanolase project (PRIN 2012).

177 References

- 178 1 Diederik S Wiersma. Disordered photonics. *Nature Photonics*, 7(7):188–196, 2013.
- 179 2 Ping Sheng. *Introduction to Wave Scattering, Localization and Mesoscopic Phenomena*. Springer,
180 1995.
- 181 3 E Akkermans and G Montambaux. *Mesoscopic physics of electrons and photons*, 2007.
- 182 4 Matteo Burrelli, Lorenzo Cortese, Lorenzo Pattelli, Mathias Kolle, Peter Vukusic, Diederik S
183 Wiersma, Ullrich Steiner, and Silvia Vignolini. Bright-White Beetle Scales Optimise Multiple
184 Scattering of Light. *Scientific Reports*, 4:1–7, August 2014.
- 185 5 S Caixeiro, M Peruzzo, and O D Onelli. Disordered Cellulose-Based Nanostructures for
186 Enhanced Light Scattering. *ACS Applied Materials & Interfaces*, pages 7885–7890, 2017.
- 187 6 J Syurik, G Jacucci, O D Onelli, Hendrik Hölscher, and S Vignolini. Bio-inspired Highly
188 Scattering Networks via Polymer Phase Separation. *Wiley Online Library*.

- 189 7 Julia Syurik, Radwanul Hasan Siddique, Antje Dollmann, Guillaume Gomard, Marc
190 Schneider, Matthias Worgull, Gabriele Wiegand, and Hendrik Hölscher. Bio-inspired, large
191 scale, highly-scattering films for nanoparticle-alternative white surfaces. *Scientific Reports*, 7:
192 srep46637, April 2017.
- 193 8 Matti S Toivonen, Olimpia D Onelli, Gianni Jacucci, Ville Lovikka, Orlando J Rojas, Olli Ikkala,
194 and Silvia Vignolini. Anomalous-Diffusion-Assisted Brightness in White Cellulose Nanofibril
195 Membranes. *Advanced materials (Deerfield Beach, Fla.)*, 30(16):e1704050, April 2018.
- 196 9 P Vukusic, B Hallam, and J Noyes. Brilliant Whiteness in Ultrathin Beetle Scales. *Science*, 315
197 (5810):348–348, January 2007.
- 198 10 Stephen M Luke, Benny T Hallam, and Peter Vukusic. Structural optimization for broadband
199 scattering in several ultra-thin white beetle scales. *Applied Optics*, 49(22):4246–12, 2010.
- 200 11 Benny T Hallam, Anthony G Hiorns, and Peter Vukusic. Developing optical efficiency through
201 optimized coating structure: biomimetic inspiration from white beetles. *Applied Optics*, 48(17):
202 3243–3249, June 2009.
- 203 12 Lorenzo Cortese, Lorenzo Pattelli, Francesco Utel, Silvia Vignolini, Matteo Burrelli, and
204 Diederik S Wiersma. Anisotropic Light Transport in White Beetle Scales. *Advanced Optical
205 Materials*, 3(10):1337–1341, June 2015.
- 206 13 Bodo D Wilts, Xiaoyuan Sheng, Mirko Holler, Ana Diaz, Manuel Guizar-Sicairos, Jörg
207 Raabe, Robert Hoppe, Shu-Hao Liu, Richard Langford, Olimpia D Onelli, Duyu Chen,
208 Salvatore Torquato, Ullrich Steiner, Christian G Schroer, Silvia Vignolini, and Alessandro Sepe.
209 Evolutionary-Optimized Photonic Network Structure in White Beetle Wing Scales. *Advanced
210 materials (Deerfield Beach, Fla.)*, 30(19):e1702057, May 2018.
- 211 14 A. Kienle, F. K. Forster, and R. Hibst. Anisotropy of light propagation in biological tissue. *Opt.
212 Lett.*, 29(22):2617–2619, Nov 2004.
- 213 15 Alwin Kienle, Cosimo D’Andrea, Florian Foschum, Paola Taroni, and Antonio Pifferi. Light
214 propagation in dry and wet softwood. *Opt. Express*, 16(13):9895–9906, Jun 2008.
- 215 16 P. M. Johnson, Sanli Faez, and Ad Lagendijk. Full characterization of anisotropic diffuse light.
216 *Opt. Express*, 16(10):7435–7446, May 2008.
- 217 17 Ad Lagendijk Patrick M. Johnson. Optical anisotropic diffusion: new model systems and
218 theoretical modeling. *Journal of Biomedical Optics*, 14:14 – – 9, 2009.
- 219 18 Lorenzo Pattelli, Romolo Savo, Matteo Burrelli, and Diederik S Wiersma. Spatio-temporal
220 visualization of light transport in complex photonic structures. *Light: Science & Applications*, 5:e16090.
221
- 222 19 Riccardo Sapienza, Sushil Mujumdar, Cecil Cheung, A G Yodh, and Diederik Wiersma.
223 Anisotropic Weak Localization of Light. *Physical Review Letters*, 92(3):033903–4, January 2004.
- 224 20 B P J Bret and A Lagendijk. Anisotropic enhanced backscattering induced by anisotropic
225 diffusion. *Physical Review E*, 70(3):77–5, September 2004.

- 226 21 Otto L Muskens, Silke L Diedenhofen, Bernard C Kaas, Rienk E Algra, Erik P A M Bakkers,
227 Jaime Gómez Rivas, and Ad Lagendijk. Large Photonic Strength of Highly Tunable Resonant
228 Nanowire Materials. *Nano Letters*, 9(3):930–934, March 2009.
- 229 22 Philipp Krauter, Christian Zoller, and Alwin Kienle. Double anisotropic coherent
230 backscattering of light. *Opt. Lett.*, 43(8):1702–1705, 2018.
- 231 23 Meint P van Albada and Ad Lagendijk. Observation of Weak Localization of Light in a
232 Random Medium. *Physical Review Letters*, 55(24):2692–2695, December 1985.
- 233 24 Pierre-Etienne Wolf and Georg Maret. Weak Localization and Coherent Backscattering of
234 Photons in Disordered Media. *Physical Review Letters*, 55(24):2696–2699, December 1985.
- 235 25 E Akkermans, P E Wolf, and R Maynard. Coherent Backscattering of Light by Disordered
236 Media: Analysis of the Peak Line Shape. *Physical Review Letters*, 56(14):1471–1474, April 1986.
- 237 26 S Etemad, R Thompson, and M J Andrejco. Weak Localization of Photons: Universal
238 Fluctuations and Ensemble Averaging. *Physical Review Letters*, 57(5):575–578, August 1986.
- 239 27 E Akkermans, P E Wolf, and R Maynard. Theoretical study of the coherent backscattering of
240 light by disordered media. *Journal de Physique*, 1988.
- 241 28 O L Muskens and A Lagendijk. Broadband enhanced backscattering spectroscopy of strongly
242 scattering media. *Optics express*, 2008.
- 243 29 Martin B van der Mark, Meint P van Albada, and Ad Lagendijk. Light scattering in strongly
244 scattering media: Multiple scattering and weak localization. *Physical Review B*, 37(7):3575–3592,
245 March 1988.
- 246 30 A Lagendijk, R Vreeker, and P De Vries. Influence of internal reflection on diffusive transport
247 in strongly scattering media. *Physics letters A*, pages 81–88, 1989.
- 248 31 J X Zhu, D J Pine, and D A Weitz. Internal reflection of diffusive light in random media.
249 *Physical Review A*, 44(6):3948–3959, September 1991.
- 250 32 Daniele Contini, Fabrizio Martelli, and Giovanni Zaccanti. Photon migration through a turbid
251 slab described by a model based on diffusion approximation. I. Theory. *Applied Optics*, 36(19):
252 4587–4599, July 1997.
- 253 33 M Born and E Wolf. Principles of optics: electromagnetic theory of propagation, interference
254 and diffraction of light, 2013.
- 255 34 C M Soukoulis, S Datta, and E N Economou. Propagation of classical waves in random media.
256 *Physical Review B*, 1994.
- 257 35 Erik Alerstam. Anisotropic diffusive transport: Connecting microscopic scattering and
258 macroscopic transport properties. *Phys. Rev. E*, 89:063202, Jun 2014.
- 259 36 B P J Bret and A Lagendijk. Anisotropic enhanced backscattering induced by anisotropic
260 diffusion. *Physical Review E*, 70(3):036601, September 2004.
- 261 37 A Ishimaru. *Wave Propagation and Scattering in Random Media (Academic, New York, 1978)*. Vols.
262 I and II, 1989.

- 263 38 Jenni Heino, Simon Arridge, Jan Sikora, and Erkki Somersalo. Anisotropic effects in highly
264 scattering media. *Phys. Rev. E*, 68:031908, Sep 2003.
- 265 39 Alwin Kienle. Anisotropic light diffusion: An oxymoron? *Phys. Rev. Lett.*, 98:218104, May 2007.
- 266 40 Jan Schäfer and Alwin Kienle. Scattering of light by multiple dielectric cylinders: comparison
267 of radiative transfer and maxwell theory. *Opt. Lett.*, 33(20):2413–2415, Oct 2008.
- 268 41 Alwin Kienle, Florian Foschum, and Ansgar Hohmann. Light propagation in structural
269 anisotropic media in the steady-state and time domains. *Physics in medicine and biology*, 58
270 (17):6205–6223, 2013.
- 271 42 R Kubo, M Toda, and N Hashitsume. *Statistical physics II: nonequilibrium statistical*
272 *mechanics*, 1985.
- 273 43 Eric W. Weisstein. Sphere Point Picking. *MathWorld—A Wolfram Web Resource*, March
274 <http://mathworld.wolfram.com/SpherePointPicking.html>.
- 275 44 G Marsaglia. Choosing a Point from the Surface of a Sphere. *Ann. Math. Stat.*, 43:645–646,
276 March 1972.
- 277 45 Hein L. Leertouwer, Bodo D. Wilts, and Doekele G. Stavenga. *Opt. Express*, 19(24):24061–24066,
278 Nov 2011.
- 279 46 N. Garcia, A. Z. Genack, and A. A. Lisyansky. Measurement of the transport mean free path
280 of diffusing photons. *Phys. Rev. B*, 46:14475–14479, Dec 1992.
- 281 47 Guillaume Labeyrie, Dominique Delande, Cord A. Müller, Christian Miniatura, and Robin
282 Kaiser. Coherent backscattering of light by an inhomogeneous cloud of cold atoms. *Phys. Rev.*
283 *A*, 67:033814, Mar 2003.
- 284 48 David Wilkowski, Yannick Bidel, Thierry Chanelière, Dominique Delande, Thibaut
285 Jonckheere, Bruce Klappauf, Guillaume Labeyrie, Christian Miniatura, Cord Axel Müller,
286 Olivier Sigwarth, and Robin Kaiser. Coherent backscattering of light by resonant atomic dipole
287 transitions. *J. Opt. Soc. Am. B*, 21(1):183–190, Jan 2004.

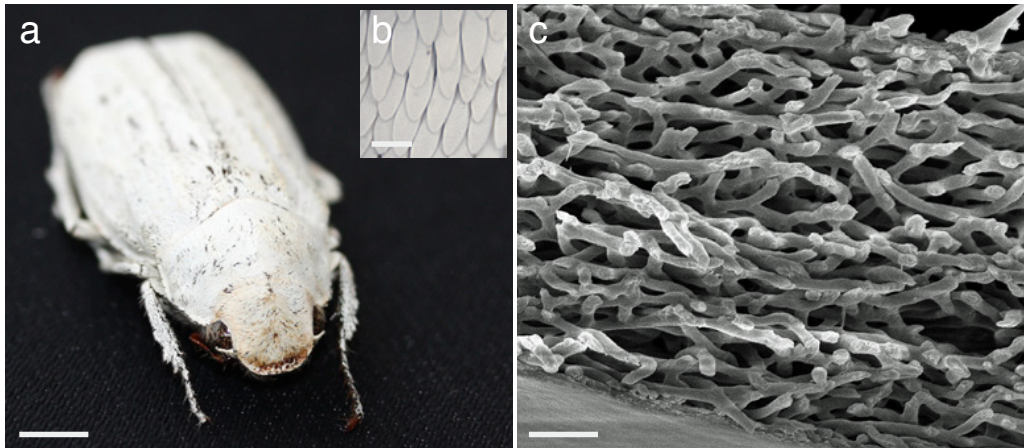


Figure 1. Images of the white beetle at different magnifications: a) photograph of the *Cyphochilus* beetle; b) micrograph of the scales organisation; c) SEM image of the cross-section of a *Cyphochilus* scale showing the interconnected network of chitin filaments which is responsible for the white appearance of the insect. Scale bar: 1 cm for a, 200 μm for b, 1 μm for c.

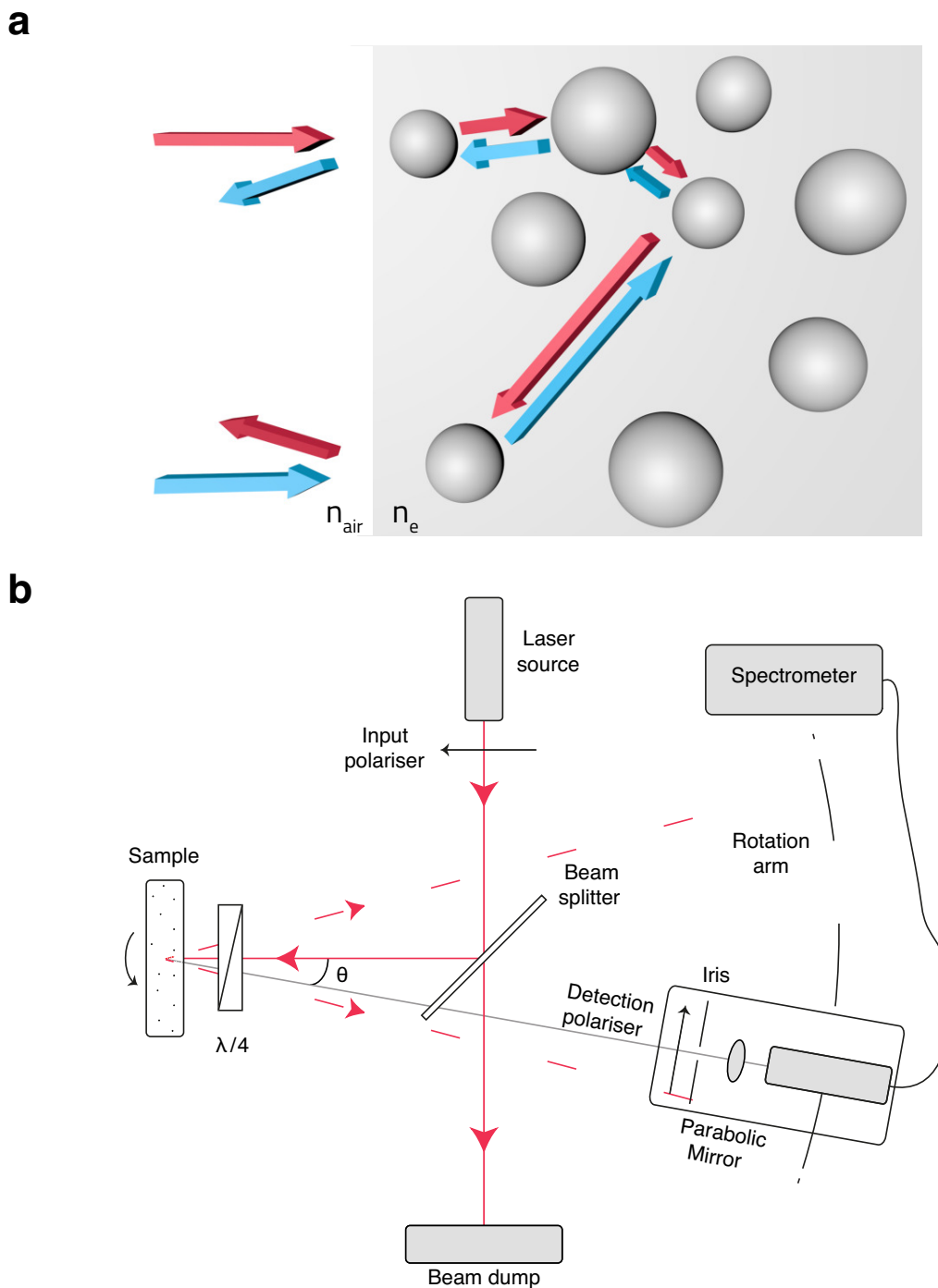


Figure 2. a) Illustration of two counter-propagating photons, red and light blue arrows. For simplicity, the scattering centers are represented as spheres. b) Schematic representation of the CBS setup in a HC configuration: the red dashed lines define the cone of backscattered intensity, while the gray line represents the detection rotation. The sample was mounted on a rotation mount, whose axis was perpendicular to the propagation direction of the laser beam, to average over different disorder realisations.

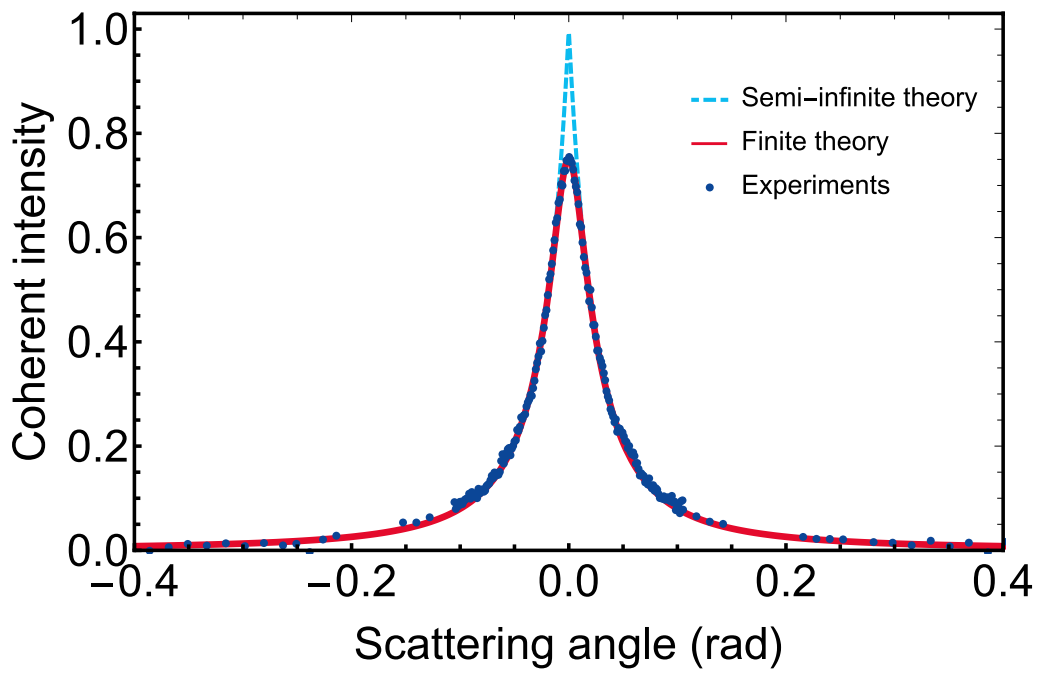


Figure 3. Theoretical fit of the experimental data (blue dots) using the isotropic theory for semi-infinite (light blue dashed line) and finite media (red solid line). Both curves were normalised to the maximum value of the semi-infinite theory. The experimental points were obtained normalising the signal measured in HC configuration to that acquired in the LNC setup.

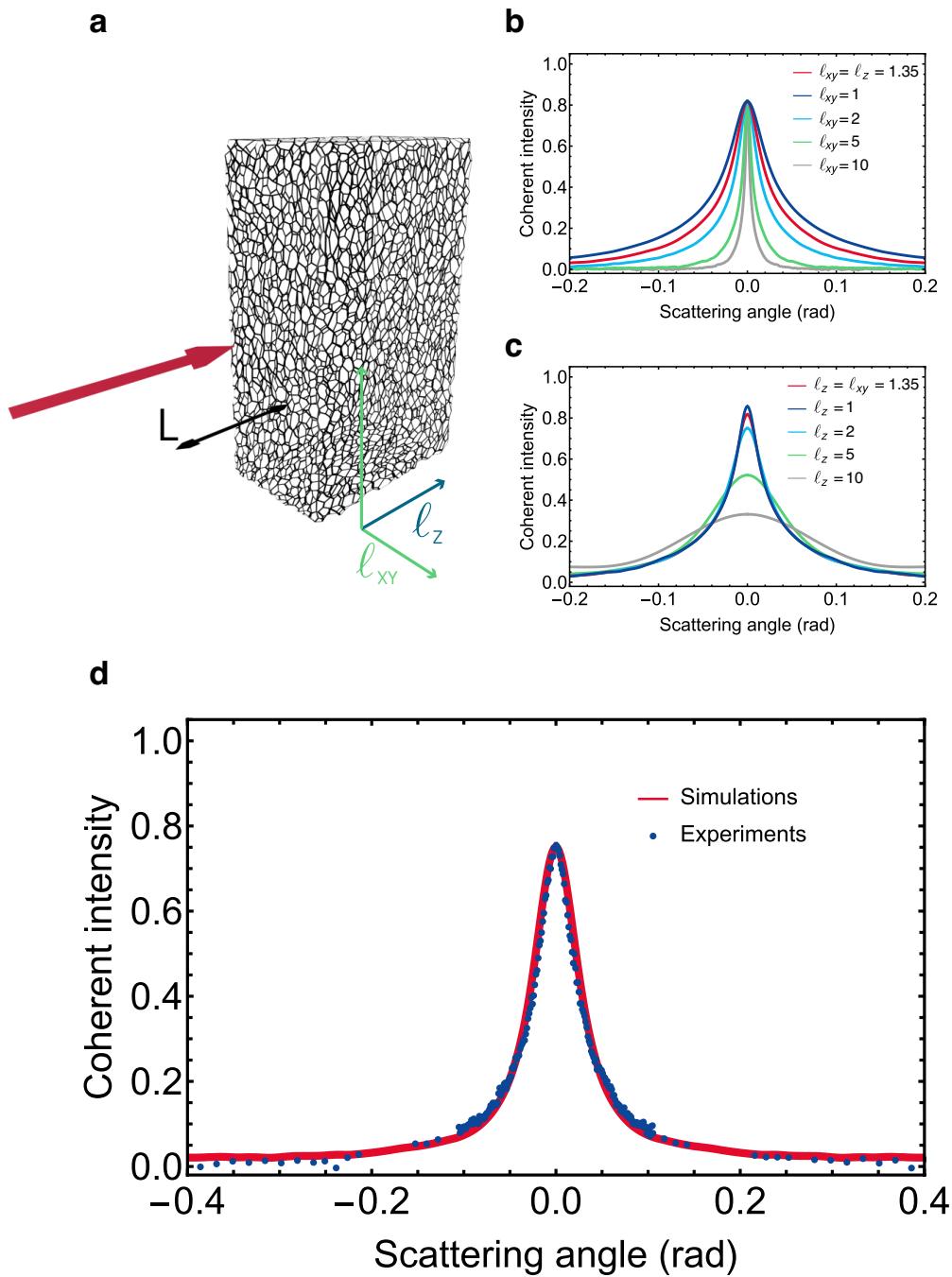


Figure 4. Monte Carlo simulation of the CBS line shape by an anisotropic medium: a) illustration of the simulation parameters, b-c) varying the in-plane components and the out-of-plane one of the mean free path. For both simulations the thickness of the slab (L) was fixed at $15\ \mu\text{m}$. d) Fit of the experimental data with the anisotropic simulation. All the simulation were performed using 1 million photons. The simulated curves were normalised to the maximum value of a simulation with $OT=1000$.